Journal of Chromatography A, 1218 (2011) 2334–2341

Contents lists available at ScienceDirect

Journal of Chromatography A

journal homepage: www.elsevier.com/locate/chroma

Evaluation of molecular mass and tacticity of polyvinyl alcohol by non-equilibrium capillary electrophoresis of equilibrium mixtures of a polymer and a dye

Enrique Javier Carrasco-Correa, Miriam Beneito-Cambra, José Manuel Herrero-Martínez, Guillermo Ramis-Ramos*

Departament de Química Analítica, Universitat de València, Dr. Moliner 50, 46100 Burjassot, Valencia, Spain

ARTICLE INFO

Article history:
Received 10 December 2010
Received in revised form 14 February 2011
Accepted 15 February 2011
Available online 22 February 2011

Keywords:
Azo-dyes
Non-equilibrium capillary electrophoresis
Polyvinylalcohol characterization
Polymer–dye complexes
Polymer molecular mass evaluation
Tacticity evaluation

ABSTRACT

Non-equilibrium capillary electrophoresis of equilibrium mixtures (NECEEM) has been used to characterize polyvinyl alcohol (PVA). Commercial PVA samples with different molecular masses, from M_w = 15 up to 205 kDa, were used. According to the ^{13}C NMR spectra, the samples also differed in tacticity (stereoregularity). Mixtures of PVA and the anionic azo-dye Congo Red (CR) were injected in the presence of a borate buffer. The electropherograms gave a band and a peak due to the residual PVA–CR complex and the excess dye, respectively, plus a superimposed exponential decay due to the partial dissociation of the complex during migration. The stoichiometry of the PVA–CR complex, q = [monomer]/[dye], reached a maximum, q_{sat}, which depended on both M_w and tacticity of PVA. Thus, q_{sat} decreased from a molar ratio of ca. 4.9 to 3.6 at increasing M_w values, this variation also being largely dependent on tacticity. A similar dependence of the electrophoretic mobility of the complex on both M_w and tacticity was also observed. A possible explanation, based on the formation of a stack of CR ions inside the PVA–CR complex, was proposed and discussed. Finally, at increasing M_w values, the stability constant of the complex increased slightly, and the pseudo-first order dissociation rate of the complex decreased, this later parameter also showing a dependence on both M_w and tacticity.

1. Introduction

A variety of nonaqueous and aqueous capillary electrophoresis (CE) methods for the characterization of synthetic polyelectrolytes, including capillary zone electrophoresis (CZE), capillary gel electrophoresis (CGE) and capillary isoelectric focusing (CIEF), have been described [1–5]. Using CE, information about size, shape, surface charge and formation of intramolecular associates can be gained [4]. Further, polyelectrolytes have been separated by CGE using solutions of nonionic polymers as sieving media [3–8]. Models describing the electrophoretic mobility of polyampholytes in free solution CZE have been developed [9], and CZE has been also used to study both the polymerization degree and the sulfonation rate of polyestyrenesulfonates [10]. Micellar electrokinetic chromatography (MECK) has been used to characterize highly charged polysaccharides (heparins) [11], and polyacrylic acids [12], as well as to study the synthesis progress and composition of ionic copolymers [13]. However, the characterization of non-charged polymers using CE has been scarcely investigated. In this connection, polyethylene glycols have been analyzed by CZE previous derivatization with an anhydride, which provides chromophore groups and electrical charges at both polymer ends [14,15]. In a previous work [16], we described a CZE method to characterize and evaluate poly(vinylpyrrolidone) (PVP); for this purpose, we used the azo-dye Congo Red (CR) which forms a charged and colored PVP–CR complex. The electropherograms of PVP–CR mixtures were interpreted at the light of the theory of non-equilibrium CE of equilibrium mixtures (NECEEM), which was developed by Krylov et al. [17–22] to obtain information about proteins and DNA fragments using fluorescent markers.

Polyvinyl alcohol (PVA) is a synthetic polymer which is widely used for a variety of purposes within the fields of cosmetic, pharmaceutical and food technologies. Depending on the route of synthesis, PVA with a different tacticity is obtained. Tacticity or stereoregularity is a characteristic feature of those polymers which have repeating adjacent chiral centers along the main chain. Tacticity depends on the class percentages of pairs of adjacent monomers or diads. The two possible classes of diads are: *m* or meso (with the same orientation) and *r* or racemic (with opposite orientation). Accordingly, three classes of units constituted by three adjacent monomers or triads can exist: *mm*, *mr* and *rr*. The relative percentages of *mm*, *mr* and *rr* triads, established by ^{1}H NMR, or

* Corresponding author. Tel.: +34 96 354 3003; fax: +34 96 354 4436.
E-mail address: ramis@uv.es (G. Ramis-Ramos).

0021-9673/$ – see front matter © 2011 Elsevier B.V. All rights reserved.
doi:10.1016/j.chroma.2011.02.040

preferably by ^{13}C NMR, are normally used to evaluate PVA tacticity [23–27].

As far as we know, CE methods for PVA characterization have not been reported, and the possibility of evaluating the tacticity of polymers using CE methods has not been investigated either. In this work, we have applied the NECEEM principles to the study of the electropherograms obtained by injecting PVA–CR mixtures. The formation of complexes between PVA and azo-dyes has been known for decades [28–32]. When excess borate was added to both the injected PVA–CR mixtures and the background electrolyte (BGE), the expected NECEEM pattern for a mixture of a non-charged macromolecule and a charged marker was obtained. Commercial PVA samples with different molecular masses, also differing in tacticity, were studied. The electropherograms of PVA–CR mixtures provided information about the electrophoretic mobility, maximal stoichiometry, thermodynamic stability constant and pseudo first-order dissociation rate constant of the PVA–CR complex. These parameters were observed to depend on both molecular mass and tacticity of PVA.

2. Experimental

2.1. Reagents

PVA samples having the following average molecular masses (M_w) and percentages of residual acetylated monomers ($n_{ac} \times 100\%$, given between parenthesis) were used: 15 (0.0%), 49 (0.1%) and 100 (12.5%) kDa (Fluka, Buchs, Switzerland), and 31 (10.8%), 61 (1.5%), 130 (10.8%), 145 (0.6%) and 205 (10.8%) kDa (Sigma–Aldrich, Steinheim, Germany). Congo Red (CR) (Panreac, Barcelona, Spain), sodium tetraborate decahydrate (borax, Sigma–Aldrich), acetone as electro-osmotic flow (EOF) marker (Scharlau, Barcelona, Spain), deuterated dimethyl sulfoxide (DMSO-d_6, Sigma–Aldrich), and other analytical grade reagents, as well as deionized water (Barnstead deionizer, Sybron, Boston, MA, USA), were also used.

2.2. Instrumentation and procedures

An HP3D CE system (Agilent Technologies, Waldbronn, Germany) provided with a diode-array detector, and uncoated fused-silica capillaries (Polymicro, Phoenix, AZ, USA) of 33.5 cm (25 cm effective length) × 50 μm I.D. (375 μm O.D.), were used. New capillaries were successively flushed with 1 and 0.1 M NaOH and water at 60 °C for 10 min each. Daily before use, the capillary was successively rinsed with 0.1 M NaOH and water for 5 min each, followed by the running BGE for 10 more minutes. After each working day, the capillary was successively flushed with water, 0.1 M HCl (10 min each), water (5 min) and NaOH 1 M, followed by more water (20 min each). Between runs, it was flushed with 0.1 M NaOH and water for 2 and 3 min, respectively, followed by the BGE for 5 more minutes. The BGE, containing 25 mM borax, was adjusted to pH 9.0 with 0.1 M HCl. Before injection, all solutions were passed through 0.45 μm pore-size nylon filters (Albet, Barcelona, Spain); however, solutions containing PVA were injected without filtering to avoid retention of the polymer by the filter material. Triplicate injections at 50 mbar × 3 s were always performed throughout all this work. Separations were conducted at 25 °C using 15 kV. Detection was set at 500 nm, close to the maximum of the absorption band of the dye in the absence of PVA; however, full spectra were also stored.

Stock solutions of the azo-dye (5 mM) and the PVA samples (10 mg mL^{-1}, 227 mM in monomers), and their mixtures, were prepared and diluted with the appropriate buffer solutions. To record UV–vis absorption spectra with the CE instrument, the capillary was filled up with 20 mM borax solutions also containing 4 mM CR and increasing PVA concentrations (49 kDa sample). The spectra were compared with those obtained with a model 8453 UV–vis spectrophotometer (Agilent Technologies) provided with a 1 mm quartz cell (Hellma, Müllheim, Germany). For this purpose, the solutions were diluted to 1:40 (0.1 mM CR). The pre-equilibration time of the PVA–CR complexes was also studied by both spectrophotometrically and CZE.

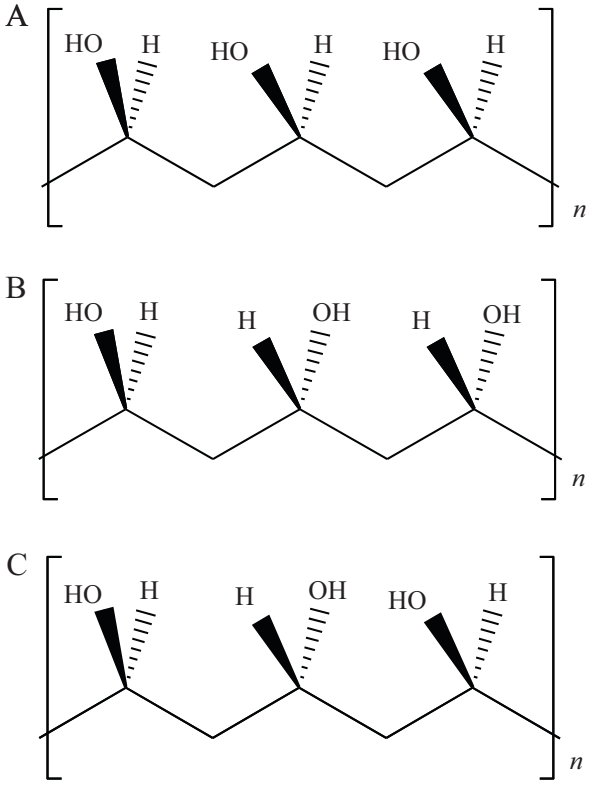

Fig. 1. The three possible classes of triads in a PVA chain: (A) *mm*, (B) *rm* and (C) *rr*.

2.3. NMR evaluation of the tacticity of the PVA samples

The tacticity (stereoregularity) of the PVA samples was established by recording the ^{13}C NMR spectra with an Ultrashield DRX 400 NMR spectrometer (Bruker, Silberstreifen, Germany). For this purpose, the PVA samples were dehydrated in a centrifugal vacuum evaporator for 8 h at 60 °C (MiVac, Genevac, Ipswich, UK); then, DMSO-d_6 to prepare 1% PVA solutions was added and sonication was applied; in all cases, 2×10^4 spectra were accumulated. The structures of the three possible *mm*, *mr* + *rm* and *rr* triad classes in a PVA chain are depicted in Fig. 1. The percentages of triad classes were estimated from the relative areas of the three multiplets found within the ca. 64–69 ppm range [24–27]. In Fig. 2, the *rr* triad percentages found in the samples are plotted against the *mm* triad percentages. In the same figure, several literature data are also given [24–27]. As observed in this figure, the PVA samples showed different tacticities, with *rr*/*mm* ratios ranging from 1.72 to 1.39 for a group of three samples, from 1.09 to 1.04 for another group of three samples, and finally, the two samples with the largest molecular masses showed the lowest *rr*/*mm* ratios, namely, 0.85 and 0.71. To facilitate the discussion that follows, these groups were qualitatively named according to the *rr*/*mm* ratio as H (high), M (medium) and L (low).

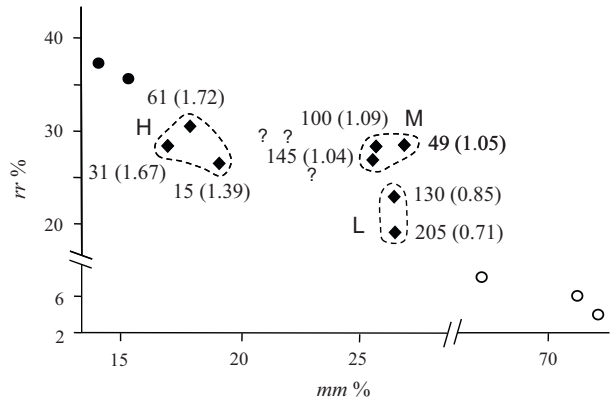

Fig. 2. Percentages of *rr* and *mm* triads found in the PVA samples used in this work (♦), as estimated by ^{13}C NMR. The numbers at the diamonds are molecular masses (kDa) and *rr*/*mm* ratios (these within parenthesis). Other symbols correspond to the literature data [24–27] for highly syndiotactic (●), atactic (▲) and highly isotactic (○) PVA.

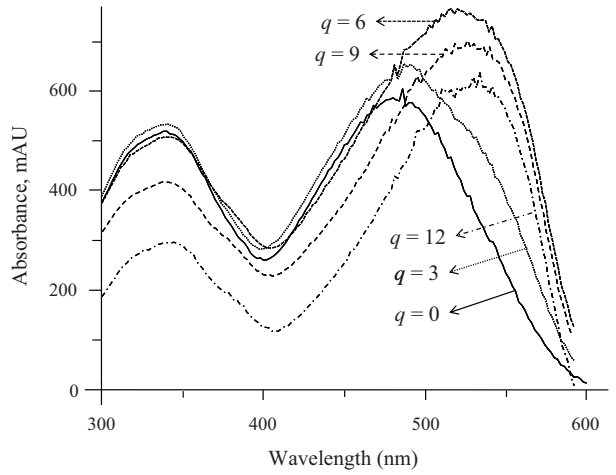

Fig. 3. UV–vis absorption spectra obtained by filling the capillary with solutions containing 20 mM borax, 4 mM CR and the following PVA concentrations (49 kDa): 0, 12, 24, 36 and 48 mM (the resulting *q* values are indicated on the traces).

3. Results and discussion

3.1. Effect of PVA on the UV–vis absorption spectrum of CR

The formation of PVA–CR complexes has been described [28–32]. As indicated in Section 2.2, the formation of the complexes was first studied by filling the capillary with PVA–CR mixtures containing 20 mM borax. As illustrated in Fig. 3 for the 49 kDa PVA sample, the UV–vis spectrum of a 4 mM CR solution was largely modified when the mixture also contained increasing PVA concentrations. Thus, from q = [monomer]/[dye] = 0 to 6, the molar absorptivity at the maximum of the main absorption band increased in a ca. 30%, and a large bathochromic shift of about 40 nm was also observed (from 479 to 519 nm). Similarly, an intensity increase of ca. 55% and a bathochromic shift of ca. 50 nm (from 489 to 539 nm) were observed with a conventional spectrophotometer when 0.4 mM PVA was added to a 0.1 mM CR solution (spectra not shown). This implies a major change in the physico-chemical environment of CR [33]. The large modification of the CR spectrum could be partially due to replacing of water molecules attached to the polar locations of CR by the polar groups of the polymer; however, as discussed below in Section 3.4, another possible reason is the stacking of dye ions in proximity to each other within the structure of the PVA–CR complex. An absorptivity decrease at all wavelengths was also observed when $q > 6$. This could be due to an increase of the refraction index of the solution or to the optical screening of the dye in the presence of a large polymer excess.

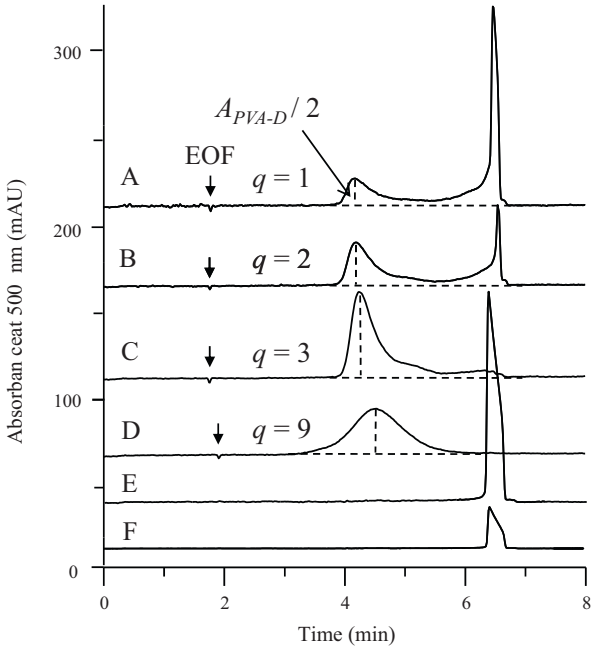

Fig. 4. From A to D: electropherograms of mixtures of CR (4 mM) and PVA (15 kDa, increasing concentrations). The *q* values are monomer/dye molar ratios. The procedure used to calculate $A_{PVA\text{-}D}$ (used to construct Fig. 5) is indicated on the traces. Traces E and F are electropherograms of 2.5 and 4 mM CR, respectively. The BGE contained 25 mM borax (pH 9), and all the injected solutions contained 20 mM borax.

3.2. Selection of working conditions

In Fig. 4, traces A–D, electropherograms of mixtures of CR (4 mM) and PVA (15 kDa, increasing concentrations) obtained in a BGE containing 25 mM borax are given. The injected mixtures were also equilibrated with borax; however, 20 mM borax was used to preserve sample stacking. Pre-equilibration with borax improved peak repeatability. In Fig. 4, traces E and F, electropherograms obtained by injecting 2.5 and 4 mM CR solutions, respectively, in the absence of PVA, are also shown. Truncation of the peak for the 4 mM CR solution was attributed to the local concentration increase produced by stacking, followed by precipitation of the dye. Truncation of this peak was not observed when PVA was present in the injected solution with $q \geq 1$. According to the NECEEM theory, when a solution containing an uncolored macromolecule and a colored charged marker is injected into the capillary, two peaks with a superimposed exponential decay region in the middle should be observed [17–22]. Thus, in Fig. 4, traces A–D, the first band was attributed to the PVA–CR complex, and the peak that followed was assumed to be contributed by both the initial CR excess in free form and the dye released by the complex during migration (contributing mainly to the left half of the peak). As *q* increased (from traces A to D), the area of the band due to the PVA–CR complex increased, and the area of the peak due to the free dye decreased. Above $q \approx 4$ the electropherograms showed the single band of the complex, which progressively widened when *q* further increased (trace D). In addition, a BGE containing 20 mM Na_2HPO_4 (pH 10) instead of borax was tried. Mixtures containing 4 mM CR and 16 mM PVA ($q = 4$) were injected; however, a low intensity wide band due to the PVA–CR complex, and a large peak and exponential decay due to the free dye, were observed (electropherograms not shown). Thus,

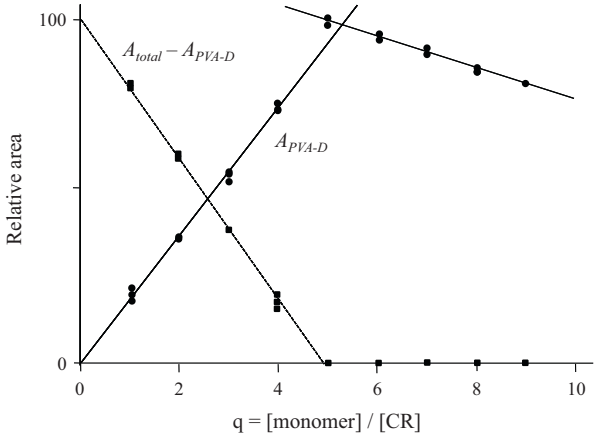

Fig. 5. Relative areas obtained from electropherograms of a series of solutions containing 4 mM CR and increasing PVA (15 kDa) concentrations in the presence of 20 mM borax. Other conditions as in Fig. 4. The continuous and dashed lines join points corresponding to the area assigned to the PVA–CR complex ($A_{PVA\text{-}D}$, estimated as indicated in Fig. 4) and the rest of the area under the peaks, respectively.

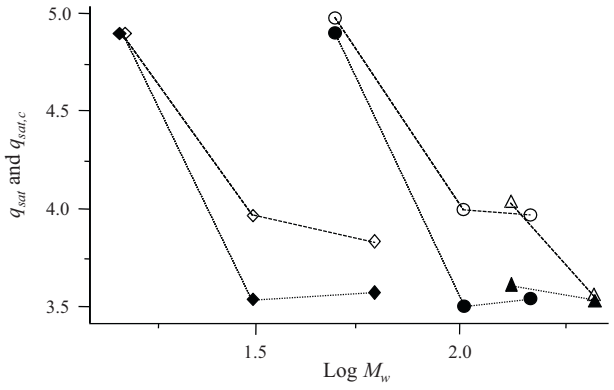

Fig. 6. Plots of the maximal stoichiometry of the complex against log M_w without (q_{sat}, full symbols) and with correction for the acetyl percentage ($q_{sat,c}$, empty symbols). Symbols indicating tacticity groups: H (diamonds), M (circles) and L (triangles).

owing to the better shape and higher intensity of the complex band, the BGE containing a borax excess was preferred.

The time required to equilibrate the mixtures before injection was studied. For this purpose, aliquots of a solution containing 20 mM borax, 4 mM CR and 16 mM PVA monomers (49 kDa, $q = 4$) were injected at regular time intervals after mixing the reagents. The area due to the remaining complex, $A_{PVA\text{-}D}$, was estimated as indicated in Fig. 4, traces A–D, by doubling the area of the left half of the complex band. The rest of the area, due to both the initial free dye and the dye released by the complex during migration, was measured as $A_{Total} - A_{PVA\text{-}D}$. A slow increase of $A_{PVA\text{-}D}$ (ca. 8%), a decrease of the rest of the area (ca. 20%), and a small increase of the electrophoretic mobility of the complex (ca. 4%), were observed during the first 2 h after mixing the reagents (sequence of electropherograms with time, not shown). This suggested a slow reorganization of the complex involving an increase of complex stability and compactness, or a decrease in its dissociation rate, or both processes at a time. Thus, to obtain reproducible electropherograms in the experiments that followed, sample injection was performed with a delay of ca. 2–3 h after mixing the reagents.

3.3. Maximal stoichiometry of the PVA–CR complex and its relationship with log M_w and tacticity

Series of electropherograms also obtained with 4 mM CR and increasing PVA concentrations (increasing q values) were used to estimate the saturation point or maximal stoichiometry of the PVA–CR complexes, q_{sat}, for all the PVA samples. As shown in Fig. 5 for the 15 kDa PVA sample, when q was increased the area of the PVA–CR complex, $A_{PVA\text{-}D}$, increased linearly up to $q \approx 4$, and the rest of the total area decreased proportionally. When $q \geq 5$, that is, above the saturation point, the peak due to the excess dye was not observed any longer, and $A_{PVA\text{-}D}$ decreased steadily. This agreed with the decrease in the absorptivity of the complex which was observed by recording spectra at large q values (Fig. 3). The other PVA samples behaved similarly, although with differences in the location of the saturation point indicating the maximal stoichiometry of the complex. In order to establish the saturation point of PVA complexes, q_{sat}, as accurately as possible, mixtures with q values close to the expected q_{sat} values were injected; however, repeatability of the electropherograms was poor when $q \approx q_{sat}$. Therefore, the q_{sat} values used in the discussion that follows were established for the different PVA samples as the point where the linear extrapolation of the decrease of $A_{Total} - A_{PVA\text{-}D}$ crossed zero (Fig. 5, dashed line).

In Fig. 6 (full symbols), the q_{sat} values obtained in this way for the PVA samples were plotted against log M_w. As observed, H samples formed a clearly resolved group with respect to the M + L samples. Also, within each tacticity group, q_{sat} decreased as log M_w increased. Further, the upper and lower limits of the q_{sat} range were similar for the H and M + L sample groups, starting at $q_{sat} \approx 4.9$ at a low molecular mass, and decreasing down to $q_{sat} \approx 3.5$ at a large molecular mass. The two L samples, which had very large molecular masses, gave both q_{sat} values close to 3.5. Thus, q_{sat} decreased from ca. 4.9 to ca. 3.5 at increasing molecular masses, but this variation took place at different log M_w values depending on tacticity.

Next, a correction of the q_{sat} values, thus to take into account the different proportions of residual acetyl groups in the PVA samples was tried. The molar proportions of residual acetyl groups per mol of monomers, n_{ac}, for the PVA samples used in this work, were given in Section 2.1. In a PVA molecule, acetyl groups could reduce the number of OH groups which are actually available to link the dye ions. Thus, in $n_{ac} \times 100\%$ acetylated PVA, only $(1 - n_{ac}) \times 100\%$ of the monomers would be available for bonding; however, this should not reduce the complexing capacity of PVA in an equivalent $(1 - n_{ac}) \times 100\%$ factor, since acetylated monomers can also perform as nonbonding bridges between bonded monomers. Nevertheless, we studied next the effect which would have on q_{sat} the extreme situation in which the complexing capacity of PVA would be reduced in a full $(1 - n_{ac}) \times 100\%$ factor. Thus, the correction applied was: $q_{sat,c} = q_{sat}/(1 - n_{ac})$. As shown in Fig. 6 (empty symbols), full correction for the acetyl percentage essentially confirmed the conclusions obtained above using uncorrected q_{sat} values concerning both the decrease of q_{sat} at increasing molecular masses and the noticeable difference between the H and M + L tacticity groups.

3.4. Structure of the complex

When $q_{sat} \approx 4.9$, each dye ion could be bonded by a maximum of four and probably a minimum of two monomers (since CR is a symmetrical structure), leaving an average of 0.9–2.9 non-bonded monomers per dye ion, respectively. Similarly, when $q_{sat} \approx 3.5$, each dye ion could be bonded by a maximum of three and a minimum of two monomers, leaving an average of 0.5–1.5 non-bonded monomers per dye ion, respectively. In both cases, a small number of non-bonded monomers are available to perform as bridges between adjacent dye ions. Thus, in all the possible scenarios, the number of non-bonded monomers per dye ion is very low, which suggests a proximity between the dye ions. As depicted in the

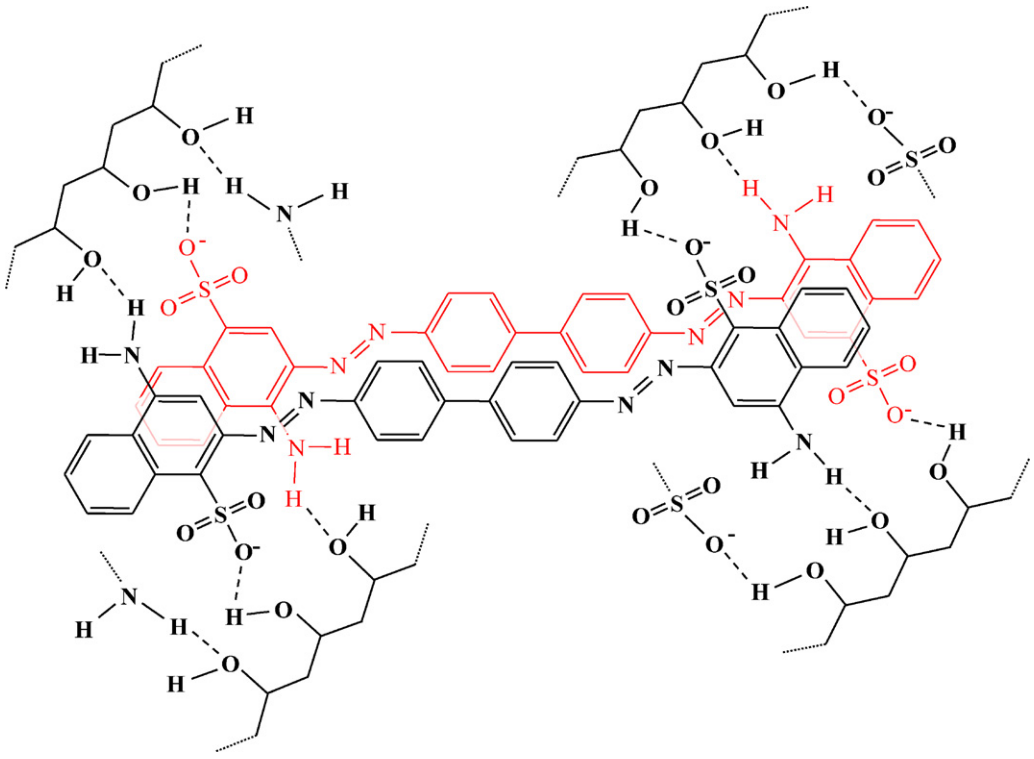

Fig. 7. Temptative structure for two adjacent PVA–CR complex units (with two stacked dye ions).

temptative structure of Fig. 7, stacks of dye ions by pairs, or by groups constituted by a higher number of dye ions, could be formed. As proposed in this figure, it seems reasonably to stack the dye ions by alternating the sulfonate and amino groups, rather than putting together all the sulfonate groups at one side and all the amino groups at the other side of the stack. Also, from a geometrical point of view, it seems reasonably to link the PVA monomers with the alternated sulfonate and amino groups though hydrogen bonds. As indicated in the literature, the azo groups are also possible sites for hydrogen bonding [30,33]; however, below the saturation point, and owing to the low stoichiometry, the number of available monomers per dye ion is rather short. Then, hydrogen bonding of the PVA monomers with both amino and azo groups, which are located in outer and inner sites of the dye ion, respectively, seems to be less likely than the structure proposed in Fig. 7. However, the probability of bonding the OH groups with azo groups should increase after the saturation point, when an excess of monomers are available.

Dye stacking, resulting in a large absorptivity increase and blue shifting of the absorption maximum, has been described in solutions of plant pigments when certain ligands and Mg^{2+} are present [34]. Thus, dye stacking could explain both the low q_{sat} values of Fig. 6 and the very large modification of the absorption spectrum when PVA is added to CR solutions (Fig. 3). Further, the distance between donor–acceptor atoms in adjacent stacked dye ions should be constricted by the distances between pairs of adjacent OH groups along the PVA chain, and these later are longer for *r* than for *m* diads. Thus, in PVA samples having a larger proportion of *r* diads, adjacent dye ions could be stacked at longer distances from each other than in samples with larger proportions of *m* diads. As discussed below, this could also explain the correlations found between other electrophoretic parameters and PVA tacticity as established by ^{13}C NMR.

The complex is probably compelled to adopt a given structure when an excess of either dye ions or unbound monomers is present. This could explain the excellent reproducibility of the electropherograms when $q < q_{sat}$ or $q > q_{sat}$, respectively. Therefore, poor reproducibility of the electropherograms when $q \approx q_{sat}$ could be due to the different ways the dye ions could be arranged within the complex when the available monomers are either in a small defect or a small excess with respect to q_{sat}.

3.5. *Influence of molecular mass and tacticity on the electrophoretic mobility of the complex*

Electropherograms obtained with PVA samples of increasing molecular mass, also corresponding to different tacticities, are shown in Fig. 8. These electropherograms were obtained with a small CR excess with respect to the saturation point. Thus, traces A and C, which correspond to complexes with $q_{sat} = 4.51$ were obtained at $q = 4$, and the other traces, which correspond to complexes with $q_{sat} = 3.51$ were obtained at $q = 3$. As further commented in Section 3.6, this was important to distinguish the A_D area from that of the exponential decay contribution, A_e. As observed in Fig. 8, the electropherograms of M + L samples (traces C–E) showed a sharper complex band than that of the H samples (traces A and B). In addition, within each tacticity group, the electrophoretic mobility of the complex was reduced at increasing molecular mass (A–B and C–D pairs). The relationships among electrophoretic mobility of the complex formed in the presence of an excess dye, molecular mass and tacticity are better recognized in Fig. 9 (full symbols). Within each tacticity group, the absolute electrophoretic mobility decreased slightly at increasing $\log M_w$ values. Therefore, electrophoretic mobilities indicated that charge density of the complexes decreased at increasing molecular masses. In addition, absolute mobility increased when the *rr*/*mm* ratio decreased between the H and M sample groups. Therefore, absolute mobility increased when the average distances between the OH groups of adjacent monomers decreased as a result of the reduction of the proportion of *r* diads, probably giving rise to an increase of complex compactness.

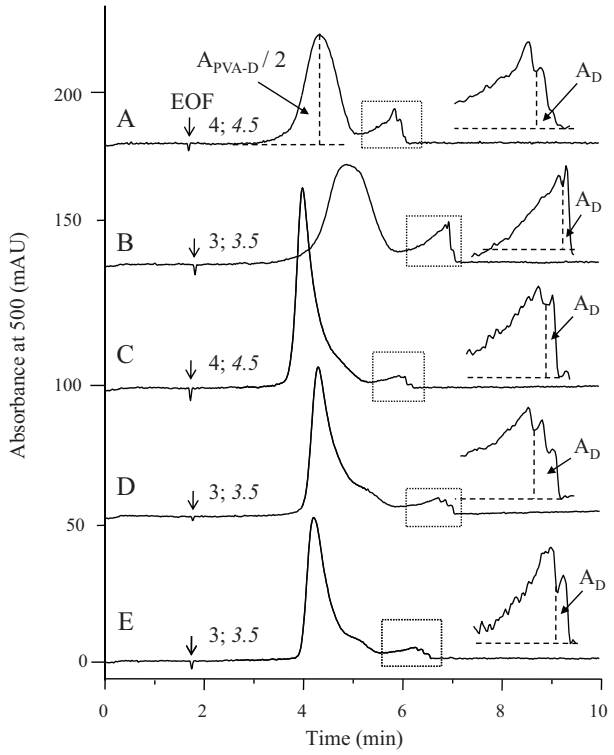

Fig. 8. Electropherograms of PVA–CR mixtures containing 20 mM borax, 4 mM CR and the following PVA monomer concentrations: (A, C) 16 mM and (B, D, E) 12 mM. The molecular masses were: (A) 15, (B) 31, (C) 49, (D) 100 and (E) 205 kDa. Sample tacticities: H (A, B), M (C, D) and L (E). The numbers on the traces are q and q_{sat} values (in italics). The expanded parts show how the A_D areas were estimated; $A_{PVA\text{-}D}$ values were estimated as indicated in trace A. Other conditions as in Fig. 4, traces A–D.

In free solution, the electrophoretic mobility of polyelectrolytes with the same linear structure but with different molecular masses is very similar [2,9,10]. This is due to the almost identical charge-to-volume ratio which is achieved when units with a given charge-to-volume ratio are increasingly added to the polyelectrolyte. This electrophoretic behavior of polyelectrolytes has been called the free draining regime [10]. As occurs with polyelectrolytes, the mobility of the PVA–CR complexes could also reach a constant value at increasing molecular masses, not further dependent on the molecular mass of PVA. However, in the case of the PVA–CR complexes formed in the presence of an excess CR, to increase the molecular mass of the polymer is not the only factor

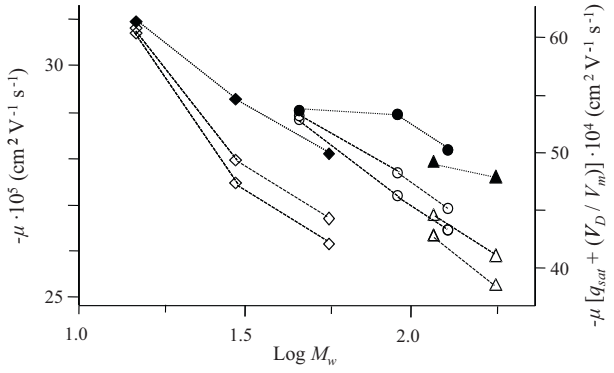

Fig. 9. Electrophoretic mobility of the PVA–CR complex against $\log M_w$, without (full symbols, dotted lines and axis at the left) and with correction for the complex stoichiometry (empty symbols, dashed lines and axis at the right); correction was performed with both $V_D/V_m = 15$ and 10. Symbols indicating tacticity groups: H (diamonds), M (circles) and L (triangles). Other conditions as in Fig. 8.

to be taken into account for a free draining regime to be reached. At increasing molecular masses, both the stoichiometry and the apparent charge density of the saturated complex, q_{sat}, should be also maintained constant. As discussed above in Section 3.3, stoichiometry of the complex formed in an excess dye varied with both molecular mass and tacticity; however, to show if a free draining regime is approached at high molecular masses, a model taking into account the stoichiometry variations can be constructed. For this purpose, the concept of average electrophoretic mobility per complex unit, μ_{unit}, can be used. This parameter was defined as the mobility due to a unit constituted by a single dye ion and the average number of monomers directly attached to that ion, plus the average share of monomers which are necessary to link the complexed dye ion to the neighboring complex units. The mobility per complex unit, μ_{unit}, should be directly proportional to the charge of a dye ion, 2, and inversely proportional to the volume of the complex unit:

$$\mu_{unit} = \frac{2f}{V_D + q_{sat}V_m} \quad (1)$$

where f is a coefficient of proportionality, V_D is the volume of a dye ion bound to the polymer chain, and V_m is the average volume of a monomer in the complex. If both sides of Eq. (1) are multiplied by the electrophoretic mobility of the complex, μ, and the equation is reorganized, we have:

$$\frac{2f\mu}{V_m\mu_{unit}} = \mu[q_{sat} + (V_D/V_m)] \quad (2)$$

Therefore, if a free draining regime would be reached at large molecular masses, the product $\mu\ [q_{sat} + (V_D/V_m)]$ would also reach a constant value. Since the V_D/V_m ratio was unknown, two approximations were used: first, V_D/V_m was taken as the ratio of the molecular masses of the dye ion and the monomers, $651/44 \approx 15$, and second, V_D/V_m was taken as the ratio of the total number of C, H, O and N atoms involved, $68/7 \approx 10$. These two values of V_D/V_m are rough approximations; however, as shown below, the use of any of them led to essentially the same conclusions. In Fig. 9 (empty symbols), product $\mu\ [q_{sat} + (V_D/V_m)]$ was plotted against $\log M_w$. As observed in this figure, the differences among tacticity groups were enhanced upon correction of the electrophoretic mobility of the complex by the effects of complex stoichiometry. This correction confirmed the independent reduction of the absolute mobility at increasing $\log M_w$ values for the H and M + L tacticity groups. Therefore, both a higher molecular mass and a higher *rr*/*mm* ratio implied a larger volume of the monomer–dye complex units, that is, a smaller packing density of the complex. This agreed with the longer distances between the OH groups in *r* diads compared to *m* diads. On the other hand, the corrected mobilities of Fig. 9 also indicated that the complex did not reach a free draining regime at increasing molecular masses. This meant that coefficient f in Eq. (2) was not constant within any molecular mass range, that is, packing density of the complex decreased at increasing molecular masses for all the PVA samples used in this work.

3.6. Stability and dissociation rate constants of the complex

In Fig. 8, it can be also observed that the area of the peak due the free dye was larger for the H (A and B traces) than for the M + L (C–E traces) tacticity groups. This indicated either a higher complex stability or a slower dissociation rate, or both features at a time, for the H group in comparison to the M + L groups. Thus, next the stability and dissociation rate constants of PVA–CR complexes were estimated. For this purpose, three areas are needed: (i) $A_{PVA\text{-}D}$, due to the PVA–CR complex; (ii) A_D, due to the free dye present in the initial equilibrium conditions; and (iii) A_e, generated by the dye released by the complex during migration. In the electrophero-

grams of Fig. 4, A_D could not be distinguished from A_e. This was attributed to the use of q values far from the maximal stoichiometry of the complexes, q_{sat}. Thus, the free dye concentration should be very low at large values of q, and conversely, at low q values, the large initial concentration of the free dye made also difficult to distinguish its contribution from that due to the dye released during complex migration. However, as shown in the expanded regions of the electropherograms of Fig. 8, at q values slightly lower than q_{sat}, it was possible to distinguish between these two contributions. Therefore, the maximum of the PVA–CR complex peak was located, and as indicated in the same figure (trace A), the area of the left half of the band was taken as $A_{PVA\text{-}D}/2$. In this band half, the contribution to the area due to the dye released during migration was assumed to be negligible (since the free dye migrates towards increasing migration times). Then, the area at the right of the first depression of the free dye peak (see the expanded parts in Fig. 8) was assigned to A_D, and A_e was calculated as the total area minus the contributions of the complex and initially free dye: $A_e = A_{Total} - (A_{PVA\text{-}D} + A_D)$. These assignments probably implied a systematic error in the estimation of A_D, and therefore also in the calculation of the stability constants; however, this made possible to compare the constants obtained with the different PVA samples. To estimate stability constants, the equilibrium molar concentration of free dye, $[D]_{eq}$, was obtained as:

$$[D]_{eq} = \frac{A_D}{b\varepsilon_D} \tag{3}$$

where $b\varepsilon_D$ is the optical path multiplied by the molar absorptivity of the dye. The equilibrium molar concentration of the complex is given by:

$$[PVA\text{-}D]_{eq} = \frac{A_{PVA-D}}{b\varepsilon_{PVA-D}} + \frac{A_e}{b\varepsilon_D} \tag{4}$$

where $\varepsilon_{PVA\text{-}D}$ is the molar absorptivity of the complex. Instead of reasoning about complex formation in terms of q_{sat} monomers per dye ion, calculations are much simpler if the formation of a 1:1 complex is assumed, being the "ligand" the complexing units formed by groups of q_{sat} monomers. The stability constant, K_s, is then given by:

$$K_s = \frac{1+R}{[C]_0(1+(1/R)) - [D]_0} \tag{5}$$

where $[C]_0$ and $[D]_0$ are the total analytical molar concentrations of the complexing polymer units and the dye, respectively, and where R is given by:

$$R = \frac{[PVA\text{-}D]_{eq}}{[D]_{eq}} = \frac{A_{PVA\text{-}D}(\varepsilon_D/\varepsilon_{PVA\text{-}D}) + A_e}{A_D} \tag{6}$$

The value of $[C]_0$ can be calculated as:

$$[C]_0 = \frac{n}{q_{sat}}[PVA]_0 \tag{7}$$

where n is the average number of monomers along the polymer chains, and where $[PVA]_0$ is the total analytical molar concentration of the polymer in mol L^{-1}. The molar absorptivity ratio $\varepsilon_D/\varepsilon_{PVA\text{-}D} = 0.77$ was obtained with a spectrophotometer at 500 nm by measuring several PVA–CR mixtures with q values sligthly lower than the respective q_{sat} values; in these conditions, the formation of a predominant complex with a 1:1 stoichiometry, in which the "ligand" was constituted by q_{sat} monomers, was assumed. In Fig. 10A, the resulting values of $\log K_s$ for $q = 2$ and 3 (full and empty symbols, respectively) were plotted against $\log M_w$. Contrary to that observed for other CZE parameters, $\log K_s$ values did not show any significant trend concerning to either molecular mass or tacticity.

The electropherograms with $q = 2$ used to obtain $\log K_s$ were further processed to estimate pseudo-first-order rate constants for the dissociation of the PVA–CR complexes. For this purpose, half-life measurements were made, and rate constants were estimated as

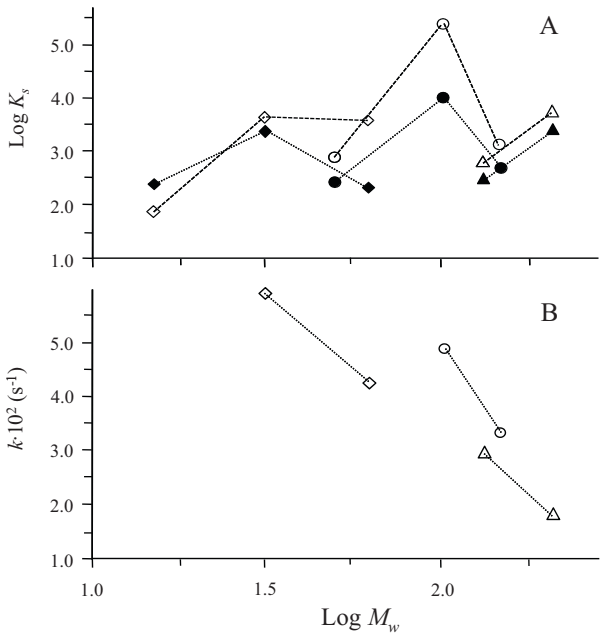

Fig. 10. Plots of (A) $\log K_s$ and (B) k vs. $\log M_w$. Data were calculated from electropherograms obtained with (A) $q = 3$ and 2 (full and empty symbols, respectively) and (B) $q = 2$. Symbols indicating tacticity groups: H (diamonds), M (circles) and L (triangles). Other conditions as in Fig. 8.

$k = \ln 2/t_{1/2}$, where $t_{1/2}$ is the half-life. The exponential decay curve within the region close to the peak of the excess dye, where the contribution of the remaining PVA–CR complex was small, was used. Five measurements of the half-life were made by selecting 5 different starting points on the decay curve of each electropherogram of series of triplicated injections. The starting points were evenly spaced from each other in about 5 s. Estimations of k were obtained with low uncertainties (ca. 4.3%). In Fig. 10B, the average values of k were plotted against $\log M_w$. Within each tacticity group, the dissociation rate constant of the complex was reduced at increasing molecular masses; in addition, H samples showed differences with respect to the M + L samples.

4. Conclusions

A PVA–CR complex is immediately formed when a PVA solution containing borate and a CR solution are mixed. Complex formation produced a large increase of the molar absorptivity and a remarkable bathochromic shift of the main band of the UV–vis absorption spectrum of CR. Using positive polarity, electropherograms of PVA–CR mixtures containing a CR excess showed the pattern predicted by the NECEEM theory for a complex formed by an uncharged macromolecule and an anionic marker. The area of the complex band increased linearly, and the areas due to the excess dye and to the dye released by the complex during migration decreased, when the PVA concentration increased up to the saturation point. The variation of the areas at increasing monomer/dye molar ratios (q values) was used to estimate the maximal stoichiometry of the complex. This ranged from $q_{sat} \sim 4.9$ to 3.5 for low and high molecular mass PVA, respectively, this variation being produced at different $\log M_w$ values depending on PVA tacticity. At the sight of the values of q_{sat}, the possible structure of the PVA–CR complex was discussed. The correlations found along this work among several electrophoretic parameters obtained in NECEEM conditions with respect to both molecular mass and tacticity of PVA can be explained by assuming that the dye ions are stacked in a proximity to each other within the struc-

ture of the PVA–CR complex. Correction of the stoichiometry taking into account the percentage of unbonding acetylated monomers ($q_{sat,c}$) confirmed the differences between tacticity groups. The shape of the PVA–CR complex band, the relative areas of the complex band and free dye peak, and the electrophoretic mobility and dissociation pseudo-first-order rate constant of the complex, were also related to both molecular mass and tacticity of PVA. Thus, the H samples gave complexes with lower absolute mobilities than the M + L samples. In comparison to M + L samples, these differences could be due to the larger distances between adjacent OH groups in H samples, which have a higher *rr*/*mm* ratio than the M + L samples. Product $\mu \cdot [q_{sat} + (V_D/V_m)]$ decreased at all molecular masses, thus indicating that a free draining regime was not reached. The variation of this product also confirmed the dependence of the mobility per complexed dye ion on tacticity. Therefore, useful information about both molecular mass and tacticity of PVA can be gained by CZE of PVA–CR mixtures. However, multivariate calibration, including the orthogonal variation of the molecular mass and *rr*/*mm* ratio values along the set of standards, would be necessary to construct multivariate models capable of making predictions of these two responses with reasonable precision. The set of commercial PVA samples we collected and used in this work was adequate to demonstrate the dependence of CZE parameters obtained in NECEEM conditions on molecular mass and tacticity, but it was deficient to support multivariate calibration. Finally, although this should be also investigated, NECEEM could be useful to evaluate molecular mass and tacticity of other soluble non-charged polymers.

Acknowledgements

Work supported by Project CTQ2010-15335 (MEC of Spain and FEDER funds). M.B.-C. thanks the Universitat de València and Químicas Oro (San Antonio de Benagéber, Spain) for a Cinc Segles-Empresa grant for PhD studies.

References

[1] H.P. Clos, H. Engelhardt, J. Chromatogr. A 802 (1998) 149.
[2] O. Grosche, J. Bohrisch, U. Wendler, W. Jaeger, H. Engelhardt, J. Chromatogr. A 894 (2000) 105.
[3] J. Borisch, O. Grosche, U. Wendler, W. Jaeger, H. Engelhardt, Macromol. Chem. Phys. 201 (2000) 447.
[4] H. Engelhardt, M. Martin, Adv. Polym. Sci. 165 (2004) 211.
[5] H. Cottet, C. Simó, W. Vayaboury, A. Cifuentes, J. Chromatogr. A 1068 (2005) 59.
[6] C.F. Welch, D.A. Hoagland, Polymer 42 (2001) 5915.
[7] M.E. Starkweather, D.A. Hoagland, M. Muthukumar, Macromolecules 33 (2000) 1245.
[8] H. Cottet, P. Gareil, J. Chromatogr. A 772 (1997) 369.
[9] D. Long, A.V. Dobrynin, M. Rubinstein, J. Chem. Phys. 108 (1998) 1234.
[10] H. Cottet, P. Gareil, O. Theodoly, C.E. Williams, Electrophoresis 21 (2000) 3529.
[11] M. Stefansson, M. Novotny, Anal. Chem. 66 (1994) 3466.
[12] J. Collet, C. Tribet, P. Gareil, Electrophoresis 17 (1996) 1202.
[13] M.R. Aguilar, A. Gallardo, J. San Roman, A. Cifuentes, Macromolecules 35 (2002) 8315.
[14] R.A. Wallingford, Anal. Chem. 68 (1996) 2541.
[15] J.P. Barry, D.R. Radtke, W.J. Carton, R.T. Anselmo, J.V. Evans, J. Chromatogr. A 800 (1998) 13.
[16] M. Beneito-Cambra, J.M. Herrero-Martínez, G. Ramis-Ramos, J. Chromatogr. A 1216 (2009) 9014.
[17] M. Berezovski, S.N. Krylov, J. Am. Chem. Soc. 124 (2002) 13674.
[18] S.N. Krylov, M. Berezovski, Analyst 128 (2003) 571.
[19] A.P. Drabovich, M. Berezovski, V. Okhoninm, S.N. Krylov, Anal. Chem. 78 (2006) 3171.
[20] X. Lin, C.L. Coyler, J. Liq. Chromatogr. Relat. Technol. 31 (2008) 1620.
[21] S.N. Krylov, J. Biomol. Screening 11 (2006) 115.
[22] S.N. Krylov, Electrophoresis 28 (2007) 69.
[23] C. Sánchez, A. Horta, Laboratorio de Macromoléculas y Técnicas de Caracterización de Polímeros, Colección Aula Abierta, UNED, Madrid, 2000.
[24] T. Moritani, I. Kuruma, K. Shibatabi, Y. Fujiwara, Macromolecules 5 (1972) 577.
[25] T.K. Wu, M.L. Sheer, Macromolecules 10 (1977) 529.
[26] R. Fukae, K. Nakata, M. Takeo, T. Yamamoto, O. Sangen, Sen'i Gakkaishi 56 (2000) 254.
[27] T.K. Wu, D.W. Ovenall, Macromolecules 6 (1973) 582.
[28] L.J. Fraunenfelder, J. Assoc. Off. Anal. Chem. 57 (1974) 796.
[29] F. Ikkai, M. Shibayama, S. Nomura, C.C. Han, Polym. Sci. 34 (1996) 939.
[30] N.J. Atkin, R.M. Abeysekera, D.H. Chenery, A.W. Robards, Polym. Sci. 39 (2001) 1471.
[31] F. Ikkai, M. Shibayama, S. Nomura, Macromolecules 27 (1994) 6383.
[32] M. Tsujimoto, M. Shibayama, Macromolecules 35 (2002) 1342.
[33] E.D. Olsen, Modern Optical Methods of Analysis, 1st ed., McGraw-Hill, New York, 1975.
[34] G.A. Ellestad, Chirality 18 (2006) 134.